# GROWTH AND TRANSPORT PROPERTIES OF TUNNELING BARRIERS IN HTS DEVICES

G. J. GERRITSMA, M. A. J. VERHOEVEN, R. MOERMAN, D. H. A. BLANK, H. ROGALLA
Applied Physics, University of Twente, P.O. Box 217, 7500 AE Enschede, Netherlands

## ABSTRACT

In this contribution we will discuss the charge transport of ramp-type HTS Josephson junctions with a Ga-doped PBCO barrier layer. It will be demonstrated that in these junctions charge transport takes place via tunneling processes. The Cooper pairs tunnel directly, at least for $T \leq T_c/2$, whereas the quasiparticles tunnel indirectly via localized states. By substituting Cu-chain atoms with Ga-atoms the density of localized states appear to be reduced, resulting in an increase in $I_cR_n$-product. Another way to increase this product is a reduction in barrier thickness. Growth studies by AFM of PBCO barriers on ramps indicate that below about 10 nm barriers become increasingly less homogeneous, and below about 6 nm pin holes are very likely to occur. This sets a lower limit on the useful barrier thickness. Presently critical-current densities up to $10^4$ A/cm$^2$ at 40 K, and $I_cR_n$-products up to 10 mV at 4.2 K are easily obtained.

## INTRODUCTION

Tunneling barriers play an important role in Josephson junctions as well as in quasiparticle injection devices. A figure of merit that characterizes a given tunnel junction, i.e. barrier and electrodes, is its $I_cR_n$-product. The upper limit of this product is eventually determined by the energy gap of the superconducting electrodes. However, in practice various factors may give rise to a considerable reduction of its value. Most junctions that have been reported in literature so far have an $I_cR_n$-product of about 1 mV or less at 4.2 K, a value that decreases by an order of magnitude at 77 K. There are, however, also some exceptions even if no excess current occurs. In the latter case the value of the $I_cR_n$-product is no longer directly related to intrinsic materials properties. These excess currents may result from pinholes in the barrier, or other inhomogeneities, but also from flux flow. The latter can be prevented by making the size of the junctions small enough. For dc-SQUID sensors these reduced values do not pose a serious problem as 1/f-noise is usually dominating at the frequencies of interest, but in digital applications higher values of the $I_cR_n$-product are of necessity in order to arrive at an acceptable noise-immunity level. If at 4.2 K Nb/Alox-junctions with a critical-current density of 1 kA/cm$^2$ are used, then at 42 K a value of 10 kA/cm$^2$ is needed. For a more detailed analyses we refer to [1] and references therein.

In the sequel we will focus our attention on junctions having a high ohmic oxide barrier of approximately the same lattice parameters as the superconducting electrodes in order to allow for fully epitaxial growth. In principle one expects that Cooper pairs as well as quasiparticles tunnel through such a barrier and that the proximity effect is absent. This tunneling is, however, not necessarily of a direct nature, and may very well proceed via so-called localized states in the barrier. This is well known for low-$T_c$ tunnel junctions, and has been extensively investigated, especially for amorphous silicon barriers [2,3]. The theory of inelastic tunneling developed by Glazman and Matveev [4] turned out to describe the



Mat. Res. Soc. Symp. Proc. Vol. 401 ©1996 Materials Research Society

observed quasiparticle transport quite well in these junctions. Therefore, one might expect that this could also be the case in high-$T_c$ (HTS) junctions with an insulating barrier having a certain amount of disorder. Given the present state in the art of thin film growth, there are plenty of defects available that could act as localized states. There presence will open up indirect tunneling channels via one, two, or more localized states that act in parallel with direct tunneling and as a result the conductance of the junction will increase. This may be written as

$$G = G_0 + G_1 + G_2 + G_3 + \cdots \quad (1)$$

Here $G$ is the total conductance, $G_0$ the contribution from direct tunneling, $G_1$ from indirect tunneling via one localized state, $G_2$ from two localized states etc. All terms are exponentially dependent on the thickness of the barrier, and we may write

$$G_n = C_n exp[-2d/(n+1)a], \quad (2)$$

where $C_n$ is a prefactor that may depend on temperature and junction bias voltage, $d$ is the thickness of the barrier and $a$ is a characteristic decay length for tunneling. In general the first two terms are independent of temperature and bias voltage, although there is a weak effect on the second term. The third and higher order terms are predominantly inelastic and hence temperature and voltage dependent. For the third and fourth term we may write

$$C_2 = C_{20}X^{4/3}, \qquad C_3 = C_{30}X^{5/2}, \quad (3)$$

where $X$=T in case eV$\ll$ kT , or $X$=V if eV$\gg$ kT, and $C_{20}, C_{30}$ are constants that depend on the details of the distribution of the localized states. From eq. 2 it is obvious that direct tunneling ($n = 0$) dominates for the thinnest barriers, and that with increasing thickness indirect tunneling processes come into play. In principle, in a given thickness range one of these processes may be the dominant charge-transport mechanism, and at a certain moment variable-range hopping (VRH) takes over [4].

Resonant tunneling of Cooper pairs via localized states has been described by Aslamazov and Fistul' [5] and was recently applied to describe the so-called long-range proximity effect that was observed in various HTS junctions [6]. As we will later demonstrate, in our junctions this does not occur, probably due to a Coulomb blockade that arises if a Cooper pair gets localized. If this happens, the Cooper pairs can only tunnel directly from one electrode to the other. Nevertheless, the critical current may be lower than what would be expected from the energy gap, or order parameter, of the bulk electrode alone. One reason is rather fundamental and is intrinsically related to the short coherence length in a HTS superconductor. Given the fact that the order parameter in the insulating barrier should be zero, this short coherence length will result in a depression of the order parameter at the interface between superconductor and insulating barrier, as was demonstrated by Deutscher and Mueller [7]. The other is also related to the short coherence length, but in a more prosaic way, i.e. if there is an interface layer that has a reduced order parameter due to defects or interdiffusion. In both cases the tunneling Cooper pairs do not come from the bulk of the electrodes, but from a region near the interface with a reduced order parameter. As a result the critical-current density will be lowered. Therefore it seems unlikely that planar sandwich junctions fabricated from c-axis oriented electrodes can have a high $I_cR_n$-product. An example is a set of trilayer junctions with Bi-2212 electrodes and Bi-22(n-1)n barriers with various dopings that were grown by atomic layer-by-layer molecular beam epitaxy. Due to the extreme smoothness of the layers grown in this fashion, monomolecular barriers could

be made that appear to be free of pinholes. Nevertheless, the $I_cR_n$-product at 4.2 K of these devices was only 0.5 mV [8]. Another reason for such a low product may be the low value of the gap in the c-axis direction.

So far, convincing experimental evidence is lacking which of the mechanisms mentioned above are responsible for the relatively low $I_cR_n$-products in HTS junctions. To that end we set out to fabricate hundreds of junctions consisting of $REBa_2Cu_3O_7$ electrodes, where RE=Y or Dy, and using $PrBa_2Ga_xCu_{3-x}O_7$ barriers with various Ga-doping levels $x$ and thicknesses $d$. The technology we used is that of the ramp-type junction that, since its inception in the spring of 1990 [9], has been considerably improved in recent years.

In the next section of this article we will analyze the growth of thin barriers on ramps and discuss its consequences. This will be followed by a section devoted to the analysis of the measured IV-Characteristics of these junctions. Finally we will draw some conclusions from the results obtained thus far.

## GROWTH ON RAMPS

Epitaxial films with the c-axis perpendicular to the substrate surface of (001) $SrTiO_3$ have been deposited using off-axis rf-magnetron sputtering in a fairly conventional way. Substrates were glued with silver paint to a stainless heater block, and outgassed in ambient at $150^0$. Next this block was brought into the sputter chamber via a load-lock system, and outgassing was continued at the deposition temperature, about $770^0$ C, until the background pressure of $10^{-6}$ mbar was achieved. As sputtering gas we used a 1:1 mixture of $Ar:O_2$ at a pressure in the range of 10-20 Pa. Deposition conditions were changed to optimize the growth of each layer separately. In order to increase the reproducibility of the layer growth, we added about one promille of water vapour to the sputter gas. Due to the increased reactivity of the sputter gas this probably prevents the target from deoxygenating in the course of time [10]. The junction fabrication process is started with the deposition of the base electrode material followed by an insulating layer, usually from the same material as the barrier. Ramps are being etched by a 500 eV argon-ion beam from a Kaufmann source, using a resist stencil to define its position. The beam hits the sample under an angle of $35^0$, whereas the actual ramp angle is about $20^0$ with the substrate surface. After removal of the resist the ramps are cleaned with the ion beam, followed *in situ* by the deposition of barrier layer and counter electrode. For further details we refer to a recent article of our group [11]. Now we may expect that the way the ramps are fabricated will lead to a heavily damaged surface layer, and one can only hope that this may be restored through diffusion and reepitaxy at the usual deposition temperature. So far, we did not try to anneal the ramps at more elevated temperatures. In order to find out how much damage actually remains, we fabricated several junctions without barrier. Even after careful optimization of the whole process the resulting critical-current density of a ramp contact is at least five times lower than that of a strip of the same dimensions. However, if the cleaning procedure was performed with a 50 eV ion beam the reduction of the critical current is only marginal. This measurement is a very sensitive indicator of any disorder in an entire plane due to a reduction of the order parameter and consequently the current that may be sustained without losses.

Using this improved cleaning procedure, we investigated the growth of thin PBCO barrier layers on these ramps by atomic force microscopy (AFM). The micrographs were taken in open air with a Nanoscope III. Commercial $Si_3N_4$ tips were used. All micrographs were recorded with at least two different tips, and checked at different scan angles to rule out

artefacts caused by tip profile. In order to enhance the details of the surface structure, we subtracted the smoothed ramps from the measurements. In fig. 1 the surface of a bare ramp can be seen. It is evident that the bare ramp has a more or less faceted, terrace-like

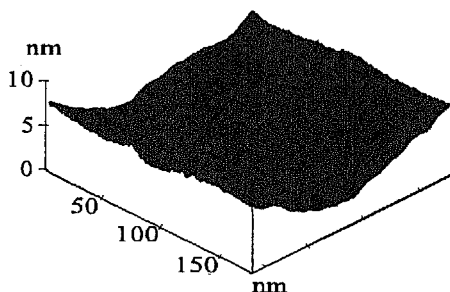


Fig.1 Overview of ramp surface morphology on an extended scale. The average ramp has been subtracted. Steps of unit-cell height can be seen.

structure. The steps that can be seen are of unit-cell height, i.e. about 1 nm. This picture does not change when a ramp is annealed at the deposition temperature for approximately one hour. In this example the ramp lies parallel to a crystallographic axis of the substrate. If this is not the case terraces are broken up, and more facets appear. In fig. 2 we present several micrographs and linescans of a ramp covered with, respectively 2, 4, and 6 nm of PBCO in going from left to right. Nucleation probably starts where facets join; they tend to cluster and give rise to oval-like structures. These structures eventually join to form long ridges separated by trenches. The surface of the covered ramp is much rougher than that of the bare ramp. The peak-to-peak height is about 10 nm. In fig. 3 we compare superimposed linescans of bare ramps with a nominally 6 nm barrier on top with those having a 10 nm barrier on top. The linescans of bare and covered ramps are shifted with respect to each other by taking notice of the average shift caused by nominal barrier thickness and ramp angle. From these and other AFM pictures that we obtained from ramps covered with barriers of various thicknesses, we infer that initially small elongated islands are formed due to nucleation of barrier material in the trenches. During the first 6 nm of growth the surface roughness increases, which is probably due to the anisotropy in the growth rate along the c-axis, respectively the ab-plane, direction. Thereafter, the ramps become smoother with increasing barrier thickness. This is probably because now the newly formed deep trenches act as nucleation sites. Growth on ramps has also be simulated by using tilted substrates. An example may be seen in fig. 4 where a HREM cross-section of a 100 nm YBCO film on a (305) $SrTiO_3$ substrate is presented. The ab-planes are tilted $31^0$ away from the substrate surface. In this case, where a film grown under non- optimized conditions is presented, anti-tilt domains are present. For optimized deposition conditions these domains are much smaller in size, and usually are only present at the interface with the substrate. On actual ramps we have never observed them. Nevertheless, the surface morphology has much in common with that of actual junctions.

What becomes immediately clear from these pictures is the fact, that barriers below

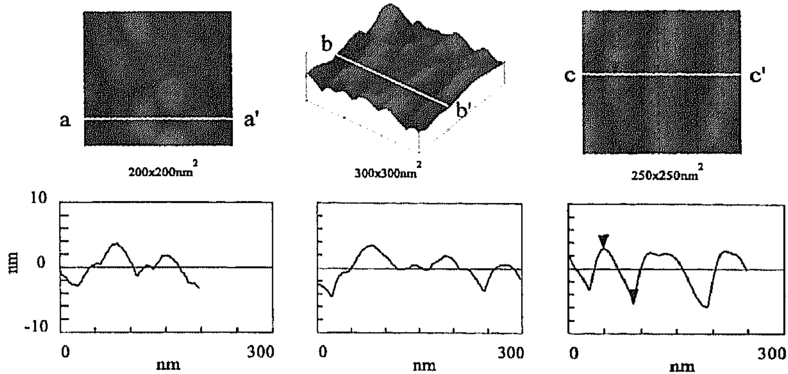


Fig.2 Ramps overgrown by a PBCO barrier. From left to right the nominal PBCO-layer thickness is 2, 4, and 6 nm, respectively. The top graphs display the surface morphology, the bottom graphs are linescans, that are indicated in the top graphs.

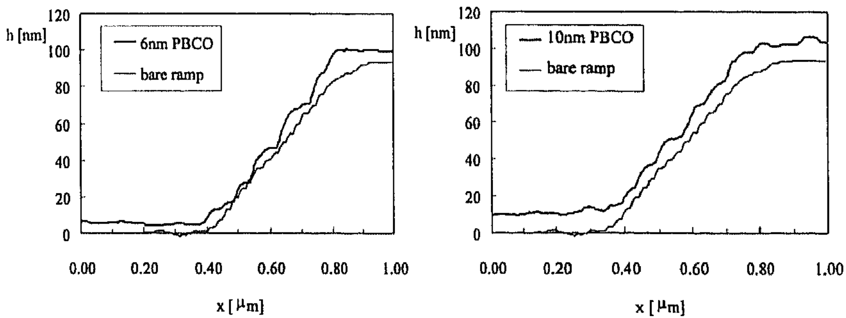


Fig.3 Linescans of ramps overgrown with 6 nm of PBCO (left), respectively 10 nm (right). In the left graph possible pinholes may be observed.

about 10 nm tend to be rather inhomogeneous in thickness, and pinholes may easily occur. This is probably the reason why junctions with a barrier below about 10 nm exhibit an increasing spread in their parameters with decreasing barrier thickness, accompanied by an increase in excess current. As a result it will be impossible to increase the $I_cR_n$- product of these junctions merely by reducing the barrier thickness. Either a barrier material should be used that is more isotropic or the deposition conditions should be modified in such a way, that initial growth starts from many nuclei and that the islands quickly coalesce before they significantly roughen the surface due the anisotropic growth rates. If a different material is

Fig.4 HREM cross-section of a 100 nm thick YBCO layer on a (305) $SrTiO_3$ substrate, simulating a $31^0$ ramp. In this example of a film grown under non-optimized conditions several anti-tilt domains are present.

required in order to decrease the barrier thickness, its characteristic tunneling distance should not be shorter than that of PBCO. Otherwise, an increase in barrier layer homogeneity may be offset by the fact that an even thinner layer would be necessary.

## BARRIER DOPING

When we started studying the influence of doping the barrier material on the IV-charac teristics of Josephson junctions, it was quite well known that doping PBCO with gallium leads to an increased resistivity of the bulk material. Up to doping levels of $x = 1.0$ the gallium atoms preferentially substitute for the copper atoms in the CuO-chains [12]. Furthermore, it is generally assumed that the charge transport in PBCO takes place in the form of VRH [13]. What we expected, of course, was an increase in junction resistance, but we did not know what would happen to the critical current. As it turned out, much to our surprise, there was no influence on the critical current by doping up to $x = 0.4$, the highest doping level we used so far [14].

We will now present the data on the normal state conductance and critical-current density of the junctions in more detail. In fig. 5 we present the critical-current density of the junctions at two temperatures and two Ga-doping levels (left), respectively, the conductance of at three Ga-doping levels (right) as function of barrier thickness. The value for the barrier thickness that we use, is the nominal thickness in the direction perpendicular to the substrate surface as inferred from the calibrated growth rate. This is not the actual distance travelled by the tunneling particles, but we simply do not know in which direction tunneling takes place. In any case all decay lengths that we obtain from the measurements are mutually comparable. What is immediately evident from the measurements is the fact, that $G$ decreases with increasing doping, as expected, but the slope, i.e. the decay length, remains constant. Furthermore, the critical- current density of the junctions does not depend on doping, neither does its slope depend on temperature. The latter only holds for temperatures below about

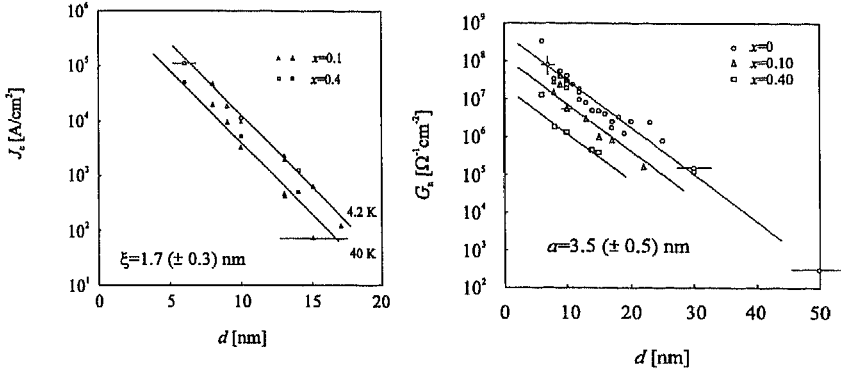


Fig.5 Critical-current density at two Ga-doping levels and two temperatures (left), respectively conductance at three Ga-doping levels (right) as function of temperature. No change in decay length is observed.

$T_c/2$. Also, a striking feature is the fact that the Cooper pair decay, or coherence, length $\xi$ and the quasiparticle decay length $a$ differ by a factor of two. This is exactly what one would expect if the former particles are tunneling directly, whereas the latter are tunneling indirectly via one localized state at 4.2 K. The fact that the Cooper pairs tunnel directly is also supported by the fact that $\xi$ is independent of temperature. In the case of a proximity effect this would not be true. The effect of Ga-doping, assuming the theory of Glazman and Matveev to be applicable, leads to a reduction in the density of localized states near the Fermi energy surface. Further evidence that this theory may hold comes from the fact that for PBCO we also observed that $G - G_{lin}$, i.e. the difference between the total conductance and the linear part, is proportional to $T^{4/3}$ at low bias voltages and to $V^{4/3}$ at high bias voltages. This is just what is predicted by Glazman and Matveev for $G_2$, and results from inelastic tunneling via two localized states. For a 50 nm thick barrier we even observed a cross-over to VRH, i.e. bulk behavior now dominates; the tunneling terms starting with $G_3$ are of minor importance. The temperature dependence of the conductance is illustrated in fig. 6, the voltage dependence in fig. 7. From this evidence we conclude that localized states in the barrier play an important role in the observed charge-transport processes in our junctions.

The microscopic origin of these states is presently unknown, nor do we know why their density is reduced by Ga-doping in the CuO-chains. The answer to this question is probably intimately connected with the absence of superconductivity, or even metallic conductivity, in PBCO. In an article by Takenaka et al. [15] in which polarized optical reflectivity spectra of untwinned PBCO in the range 0.03-40 eV are discussed, it was demonstrated that holes reside mainly in the CuO-chains (50%) and at the Pr-atom sites (50%). The latter is not a direct consequence of the measurements, but results from a charge-neutrality argument. The tendency for hole doping in the chains, in stead of the planes, finds also support from theory [16,17]. In the last reference it is demonstrated that holes from the planes may be grabbed by the so-called FR-band. The latter is assumed to be very sensitive to Pr-disorder and as a result will be nonconducting. Furthermore, Takenaka et al. observed a decrease in

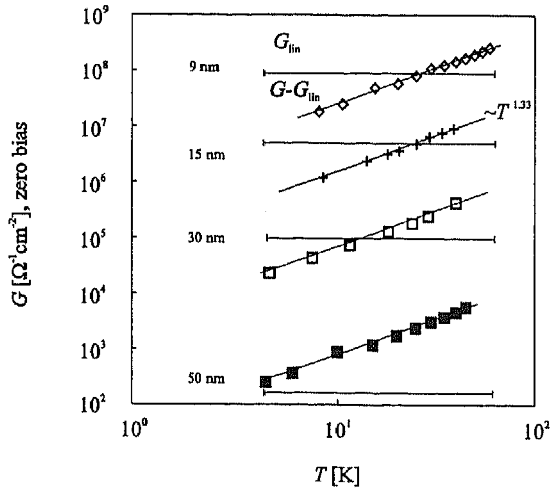


Fig.6 Non-linear part of the zero-bias conductance of PBCO as a function of temperature. The solid lines through the data points show a fit to a $T^{4/3}$-power law. The linear part is indicated by horizontal lines.

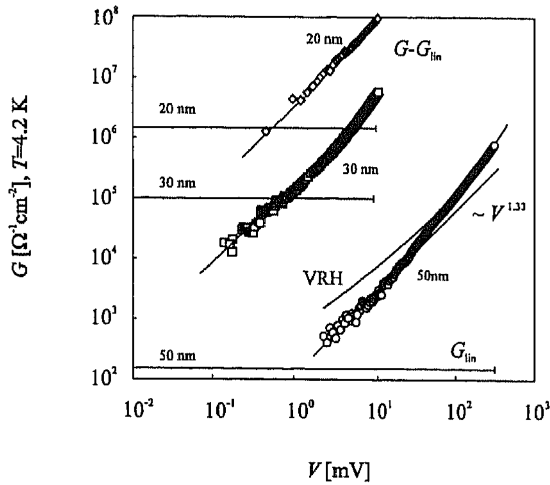


Fig.7 Non-linear part of the high-bias conductance of PBCO as a function of voltage. The solid lines through the data points show a fit to a $V^{4/3}$-power law. For a 50 nm barrier a clear cross-over to VRH may be observed. The horizontal lines indicate the linear part of the conductance.

the conductivity along the CuO-chain direction below 0.2 eV, an indication of localization of chain holes caused by disorder. The latter probably results from chain-oxygen defects. These observations are consistent with the observed semiconductive resistivity of this compound. Hence, we think it to be quite likely that if Cu-atoms with formal valence state 2.5+ are replaced by Ga- atoms with valence state 3+ the number of holes, and hence the number of localized states will be reduced. This seems to be consistent with the observed reduction in localized states that participate in the conductance. However, the situation is not so simple, for if 10% substitution has taken place, the conductance decreases by an order of magnitude and the discrepancy gets even worse at 40% substitution.

## CONCLUSIONS

As we have demonstrated, charge transport in HTS ramp-type Josephson junctions with a Ga-doped PBCO barrier is dominated by tunneling processes. The Cooper pairs tunnel directly, at least for temperatures below about $T_c/2$, whereas the quasiparticles tunnel indirectly via localized states. The density of these states may be reduced by Ga-doping, which we tested so far up to x=0.4. As this does not affect the Cooper-pair tunneling, doping results in an increase of the $I_cR_n$-product of these junctions. Presently we are able to fabricate junctions with an $I_cR_n$-product up to about 10 mV. Furthermore, critical-current densities of $10^4$ A/cm$^2$ are easily achieved. Hence, these junctions may be operated at 42 K with the same noise-immunity level as ordinary Nb/Alox tunnel junctions at 4.2 K.

What remains to be seen is, if further improvement is possible. Growth studies of PBCO barriers on ramps, so far, indicate that a reduction of the barrier thickness below about 6 nm is impossible. This sets an upper limit on the critical-current density. Furthermore, a cross-over to direct tunneling of the quasiparticles cannot be achieved in this way. To solve this problem further work is needed to see if the growth conditions may be changed to prevent the roughening of the barrier layer, or alternatively if a suitable material may be found that is less anisotropic. A route that is attractive to pursue is a further increase in doping levels. This is not necessarily restricted to PBCO. There are four 1:2:3-compounds which allow for a 100% substitution of their Cu-chain atoms by gallium, and yet reveal single-phase formation. If Co-doping is used there are even 10 single-phase compounds available [18]. If increased Ga-doping turns out to work well in reducing the density of localized states, a further increase in junction resistance, and hence $I_cR_n$-product may be expected. It will be interesting to see if in this way quasiparticles may be forced to tunnel directly, due to a lack of suitable localized states. In that case it might also be possible to observe a clear gap structure in the conductance curve.


## ACKNOWLEDGEMENT

We are indebted to dr. H.W. Zandbergen from the Centre for HREM from the Delft University of Technology for making available the HREM cross-section of YBCO on (305) $SrTiO_3$, and dr. E.M.C.M. Reuvekamp for his stimulating discussions on structure analyses. This research is in part supported by the EC, contract number ESPRIT 6677.


## REFERENCES


1. R.J. Wiegerink, G.J. Gerritsma, E.M.C.M. Reuvekamp, M.A.J. Verhoeven and H. Rogalla, IEEE Trans. Appl. Superconduct. 5, 3452 (1995).

2. Y. Xu, A. Matsuda, and M.R. Beasley, Phys. Rev. B **42**, 1494 (1990).
3. Y. Xu, D. Ephron, and M.R. Beasly, Phys. Rev. B bfseries 52, 2843 (1995).
4. L.I. Glazman and K.A. Matveev, Sov. Phys. JETP **67**, 1276 (1988) [Zh. Eksp. Teor. Fiz. **94**, 332 (1988)].
5. L.G. Aslamazov and M.V. Fistul', Sov.Phys. JETP **56**, 666 (1982) [Zh. Eksp. Teor. Fiz. **83**, 1170 (1982)].
6. I.A. Devyatov and M.Yu. Kupriyanov, JETP Lett. **59**, 200 (1994) [Pis'ma Zh. Eksp. Teor. Fiz. **59**, 187 (1994)].
7. G. Deutscher and K.A. Mueller, Phys. Rev. Lett. **59**, 1745 (1987).
8. M.E. Klausmeier-Brown, G.F. Virshup, I. Bozovic, J.N. Eckstein and K.S. Ralls, Appl. Phys. Lett. **60**, 2807 (1992).
9. J. Gao, W.A.M. Aarnink, G.J. Gerritsma and H. Rogalla, Physica C **171**, 126 (1990).
10. J.R. Gavaler, J. Talvacchio, T.T. Braggings, M.G. Forrester, J. Greggi, J. Appl. Phys. **70**, 4383 (1991).
11. M.A.J. Verhoeven, G.J. Gerritsma and H. Rogalla, IEEE Trans. Appl. Supercond. 5, 2095 (1995).
12. E. Sodtke, C. Andrzejak, D. Guggi, Y Xu, Phycica C **180**, 50 (1991).
13. B. Fisher, G. Koren, J. Genossar, L. Patlagan and E.L. Gartstein, Physica C **176**, 75 (1991).
14. M.A.J. Verhoeven, G.J. Gerritsma and H. Rogalla, IEEE Trans. Appl. Superconduct. **5**, 2095 (1995).
15. K. Takenaka, Y. Imanaka, K. Tamasaku, T. Itoh, and S. Uchida, Phys. Rev. B **46** , 5833 (1992).
16. R. Fehrenbacher and T.M. Rice, Phys. Rev. Lett. **70**, 347 (1991).
17. A.I Lichtenstein and I.I. Mazin, Phys. Rev. Lett. **74**, 1000 (1995).
18. T.A. Mary, N.R.S. Kumar, and U.V. Varadaraju, J. Solid State Chem. **107**, 524 (1993).